

Helical Structures | Hot Paper |

 **α -Aminoxy Peptoids: A Unique Peptoid Backbone with a Preference for *cis*-Amide Bonds**Viktoria Krieger,^[a] Emanuele Ciglia,^[a] Roland Thoma,^[b] Vera Vasylyeva,^[b] Benedikt Frieg,^[a] Nader de Sousa Amadeu,^[b] Thomas Kurz,^[a] Christoph Janiak,^[b] Holger Gohlke,^[a] and Finn K. Hansen^{*[a, c]}

Abstract: α -Peptoids, or *N*-substituted glycine oligomers, are an important class of peptidomimetic foldamers with proteolytic stability. Nevertheless, the presence of *cis/trans*-amide bond conformers, which contribute to the high flexibility of α -peptoids, is considered as a major drawback. A modified peptoid backbone with an improved control of the amide bond geometry could therefore help to overcome this limitation. Herein, we have performed the first thorough analysis of the folding propensities of α -aminoxy peptoids (or *N*-substituted 2-aminoxyacetic acid oligomers). To this end, the amide bond geometry and the conformational properties of a series of model α -aminoxy peptoids were investigated by using 1D and 2D NMR experiments, X-ray crys-

tallography, natural bond orbital (NBO) analysis, circular dichroism (CD) spectroscopy, and molecular dynamics (MD) simulations revealing a unique preference for *cis*-amide bonds even in the absence of *cis*-directing side chains. The conformational analysis based on the MD simulations revealed that α -aminoxy peptoids can adopt helical conformations that can mimic the spatial arrangement of peptide side chains in a canonical α -helix. Given their ease of synthesis and conformational properties, α -aminoxy peptoids represent a new member of the peptoid family capable of controlling the amide isomerism while maintaining the potential for side-chain diversity.

Introduction

α -Peptoids, or oligomers of *N*-substituted glycine, have several advantages over peptides as potential bioactive compounds including proteolytic stability and increased cell permeability.^[1,2] Peptoid libraries have been utilized as protein binding agents and as inhibitors of protein–protein interactions,^[3–6] although primary screening hits identified from peptoid libraries have usually not displayed high activity or potency.^[7] The major limitation of peptoids is the lack of conformational constraints due to the absence of internal hydrogen bonding, which may reduce their binding affinity to proteins. In contrast to peptides, a high degree of *cis*-amide bonds is observed in

α -peptoids.^[8] The *cis*- and *trans*-amide conformations are almost isoenergetic for *N*-alkyl α -peptoid monomers, and studies have shown that the nature of the side chain can significantly modulate the ratio of *cis/trans*-amide bond conformers.^[9] Nevertheless, α -peptoids can form stable, helical secondary structures when the *cis/trans*-amide isomerism is optimally controlled.

Similarly, it has been hypothesized that β -peptoids (*N*-alkyl β -alanines) can exhibit foldamer properties.^[10–14] A recent study by Olsen and co-workers provided a high-resolution X-ray crystal structure of a β -peptoid hexamer containing strongly *cis*-inducing *N*-(*S*)-1-(1-naphthyl)ethyl side chains. The crystal structure disclosed an all-*cis*-amide bond geometry and a right-handed helical conformation with exactly three residues per turn and a helical pitch of 9.6–9.8 Å between the turns.^[15] However, it is important to note that the amide bond geometry in β -peptoids is also highly dependent on the nature of the side chain.^[16]

Thus far, the control of the folding properties of α - and β -peptoids is mainly achieved by incorporation of specific *cis*- or *trans*-directing side chains. This focus on a small number of side chains comes at the expense of diversity.^[7,17] Accordingly, it is worthwhile to address this limitation and to aim at the design of peptoid backbones with an improved control of the *cis/trans*-amide isomerism. In 2002, Shin and Park reported the preparation of α -aminoxy peptoid pentamers, but the folding properties were not investigated.^[18] The backbone-controlled secondary structures of α -aminoxy peptides^[19,20] prompted us

[a] V. Krieger, Dr. E. Ciglia, B. Frieg, Prof. Dr. T. Kurz, Prof. Dr. H. Gohlke, Prof. Dr. F. K. Hansen
Institute of Pharmaceutical and Medicinal Chemistry
Heinrich-Heine-Universität Düsseldorf
Universitätsstrasse 1, 40225 Düsseldorf (Germany)

[b] R. Thoma, Dr. V. Vasylyeva, Dr. N. de Sousa Amadeu, Prof. Dr. C. Janiak
Institute of Inorganic and Structural Chemistry
Heinrich-Heine-Universität Düsseldorf
Universitätsstrasse 1, 40225 Düsseldorf (Germany)

[c] Prof. Dr. F. K. Hansen
Pharmaceutical/Medicinal Chemistry
Institute of Pharmacy, Leipzig University
Brüderstrasse 34, 04103 Leipzig (Germany)
E-mail: finn.hansen@uni-leipzig.de

 Supporting information for this article can be found under:
<http://dx.doi.org/10.1002/chem.201605100>.

to analyze the conformational properties of α -aminoxy peptoids (or oxa-analogues of β -peptoids) in detail. In this work, we report the results of our study revealing a unique *cis*-amide bond preference of α -aminoxy peptoids in comparison to other peptoid backbones.

Results and Discussion

We first designed and synthesized a series of model α -aminoxy peptoids utilizing an N-terminal acetyl and a C-terminal piperidyl cap group to investigate the influence of several side chains on the amide conformation (see the Supporting Information for synthetic details). To be consistent with the peptoid nomenclature, we use the terms "*cis*" and "*trans*" to describe the amide dihedral angle omega referring to the relative position of the backbone atoms (see Figure 1). As a consequence,

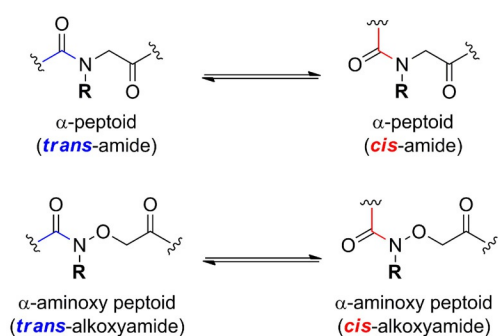


Figure 1. Selected peptoid backbones.

the *cis* conformer features an *E*-configured hydroxamate moiety, whereas the *trans* conformer corresponds to a *Z*-configured hydroxamate. The definition of all other relevant dihedral angles is outlined in Figure 2. The α -aminoxy peptoids 1 and 3–5 were designed to investigate the *cis/trans* isomerism in the absence of strongly *cis*- or *trans*-directing side chains. Compound 2 was included due to its strongly *trans*-amide

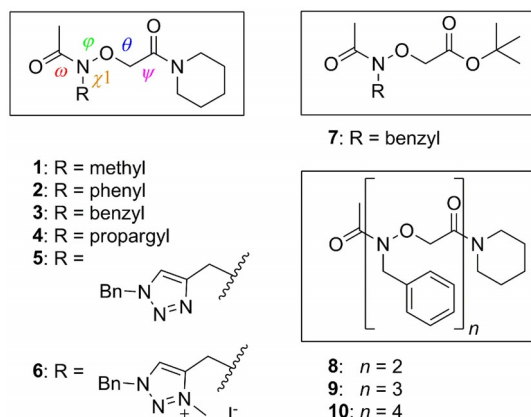


Figure 2. α -Aminoxy peptoids investigated in this study. The relevant backbone dihedral angles are defined as follows: $\omega = [\text{C}\alpha_{(i-1)}, \text{C}_{(i-1)}, \text{N}, \text{O}]$, $\varphi = [\text{C}_{(i-1)}, \text{N}, \text{O}, \text{C}\alpha]$, $\theta = [\text{N}, \text{O}, \text{C}\alpha, \text{C}]$, $\psi = [\text{O}, \text{C}\alpha, \text{C}, \text{N}_{(i+1)}]$, and $\chi_1 = [\text{NC}\beta, \text{NC}\alpha, \text{N}, \text{O}]$.

bond-inducing phenyl side chain.^[21] The α -aminoxy peptoid 6 served as a *cis*-promoting model compound due to the *cis*-directing triazolium side chain.^[17] The model peptoid 7 containing a *tert*-butyl ester was incorporated to analyze an alternative C-terminal cap group. The α -aminoxy peptoids 8–10 were synthesized as model compounds for oligomeric α -aminoxy peptoids to study the conformational preference in oligomers (see the Supporting Information for synthetic details).

We next studied the conformational homogeneity of our model systems by using standard 1D NMR techniques at room temperature. ¹H NMR spectra of the peptoid monomers 1–6 were recorded in CDCl₃ at room temperature and revealed only a single set of NMR signals. However, some signals appeared broad. We therefore collected the ¹H spectra of the monomers 1–6 in [D₃]acetonitrile, [D₄]MeOH, D₂O, and [D₆]DMSO observing again some relatively broad signals in the case of the peptoids 1–5 (see the Supporting Information). These results prompted us to study the ¹H NMR spectra in more detail. We performed variable temperature (VT) NMR experiments on the α -aminoxy peptoid 3 in CDCl₃. Cooling caused the signals of compound 3 to split into two sets of sharp signals at –20 and –30 °C in ratios of 87:13 and 86:14, respectively (Figure S1 in the Supporting Information). In order to exclude that the second species arises from the piperidyl group, we repeated the VT NMR experiment with the model α -aminoxy peptoid 7 containing a *tert*-butyl ester as the C-terminal cap. Compound 7 followed the same trend as observed for the α -aminoxy peptoid 3 (Figure S2 in the Supporting Information). To study whether the additional NMR signals arise from aggregation, we recorded the ¹H NMR spectra of compound 3 at –30 °C with varying concentrations (0.15–150 mM, Figure S3 in the Supporting Information), which showed no concentration dependency of the peak ratio. Interestingly, a VT NMR experiment with the deacetylated analogue of the α -aminoxy peptoid 3 (i.e., 2-((benzylamino)oxy)-1-(piperidin-1-yl)ethan-1-one) did not show any additional conformational peaks (Figure S4 in the Supporting Information). Thus, we reasoned the presence of two sets of NMR signals might indicate the coexistence of two well-defined species that equilibrate slowly on the NMR time scale, for example, *cis/trans*-amide bond rotamers. This hypothesis was supported by detection of EXSY signals in a 2D NOESY experiment on compound 3 in CDCl₃ at –30 °C (Figure S5 in the Supporting Information).^[22] This behavior is typical for protons under significant chemical exchange on the saturation time scale and thus implies the existence of rotamers.^[23] Subsequent ¹H NMR experiments with compounds 1, 2, and 4–6 at –30 °C provided further evidence for the existence of *cis/trans*-amide bond conformers. In the case of compounds 1, 4, and 5 we observed a similar behavior as for compound 3 with ratios^[24] of 84:16 (compound 1), 84:16 (compound 4), and 82:18 (compound 5). Notably, the ¹H NMR spectrum of the peptoid 2 (containing a *trans*-directing side chain) revealed an increased amount of the minor conformer at –30 °C in CDCl₃ (ratio of 65:35), whereas the spectrum of the α -aminoxy peptoid 6 (containing a *cis*-directing side chain) showed well-defined peaks with no evidence for a significant population of another conformer. To study the conformational

stability of longer peptoid sequences, the α -aminoxy peptoid oligomers **8–10** were synthesized (see the Supporting Information). The ^1H NMR spectra conducted in CDCl_3 , $[\text{D}_3]\text{acetonitrile}$, and $[\text{D}_4]\text{MeOH}$ showed well-defined signals (see the Supporting Information for details). The ^1H NMR spectra measured at -30°C in CDCl_3 revealed one major conformer in all cases. However, in the α -aminoxy dipeptoid **8** a second conformational isomer was observed (ratio of 86:14). In the case of the α -aminoxy tripeptoid **9** and the α -aminoxy tetrapeptoid **10** only traces of side peaks were observed.

Because several model monomers and oligomers revealed the presence of two conformers, we performed comprehensive NMR experiments on the α -aminoxy peptoid **3** in CDCl_3 to determine the Arrhenius activation energy for the rotational barrier. For this purpose, the interconversion rate constants at the respective coalescence temperatures were measured by VT NMR experiments by using different NMR instruments. A plot of the temperature dependence of the interconversion rate constants afforded the Arrhenius activation energy ($E_a = (42 \pm 2) \text{ kJ mol}^{-1}$, see the Supporting Information for details).

In order to investigate whether α -aminoxy peptoid monomers prefer *cis*- or *trans*-configured amide bonds, we decided to study the amide bond geometry of our model compounds in detail. Based on our observed side-chain dependency we assumed a *cis* preference in the case of our model α -aminoxy peptoids. To confirm a preferred *cis*-amide bond configuration in solution, the torsion angle ω was analyzed by 2D NMR spectroscopy. Compound **6** was chosen for recording a 2D NOESY NMR spectrum due to the absence of any additional conformational peaks. We observed a strong cross peak between the N-terminal acetyl group and the backbone methylene protons as well as a weak NOE between the acetyl and the side chain methylene protons (Figure S6 in the Supporting Information). We reasoned that a *cis*-configured amide ($\omega \approx 0^\circ$) would fulfill these distance requirements, whereas a *trans*-configured amide ($\omega \approx 180^\circ$) should show a stronger NOE between the acetyl and the side chain methylene protons. A 2D NOESY spectrum of the α -aminoxy peptoid **3** at -30°C revealed a strong cross peak between the N-terminal acetyl group and the backbone methylene protons for the major conformer, which indicates a *cis*-amide bond geometry (Figure S7 in the Supporting Information). Notably, our results are in good agreement with data reported from Grel and co-workers who showed that simple alkoxyamides prefer *cis*-amide bonds in the absence of hydrogen bonds.^[25] The above-mentioned data suggest that the α -aminoxy peptoid monomers **1** and **3–6** possess a strong preference for *cis*-configured amide bonds. In particular, it is worth noting that the model compounds **1** and **3–5** are showing a significant preference for *cis*-amide bonds (>80%) even in the absence of any *cis*-directing side chains. In contrast, α -peptoids bearing identical cap groups and side chains revealed inhomogeneous mixtures of *cis/trans* rotamers or even a preference for *trans*-amide bonds (Figure S8 in the Supporting Information).

Fortunately, we were able to obtain X-ray quality crystals of the α -aminoxy peptoid monomer **1** and the tripeptoid **9** by slow evaporation from a CDCl_3 solution. The X-ray structure

analysis of the α -aminoxy peptoid **1** proved a *cis*-amide configuration in the solid state. Although the *N*-methylacetamide group in the α -aminoxy peptoid **1** was disordered in the crystal structure, it is important to note that the amide is *cis*-configured in both the A and B component (Figure 3). The X-ray

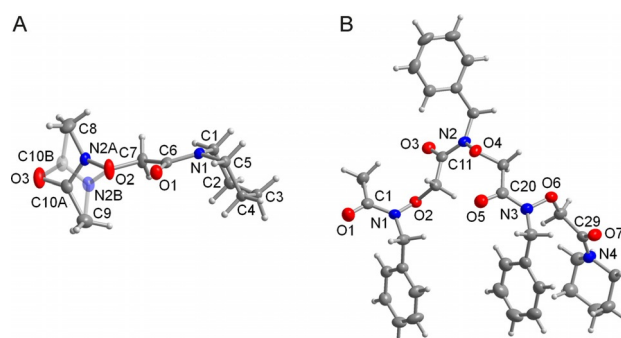


Figure 3. Thermal ellipsoid plots of A) the α -aminoxy peptoid **1** and B) the α -aminoxy tripeptoid **9** (50% probability for compound **1**, 70% probability for compound **9**, hydrogen atoms with arbitrary radii). The N and C(=O) atom of the *N*-methylacetamide group in compound **1** is disordered in a C_2 -type (180°) rotation around the O3–O2 connector with equal occupancy (see the Supporting Information for further details). One of the disordered positions is shown semi-transparent.

structure of the α -aminoxy tripeptoid **9** revealed an all-*cis*-amide geometry (Figure 3). The observed torsion angles are summarized in Table S1 in the Supporting Information. Interestingly, the N-terminal (*i*) and the internal (*i*+1) monomer disclosed almost identical backbone torsion angles, whereas the C-terminal monomer (*i*+2) showed different torsion angles. This phenomenon can be explained by packing effects in the solid state (see the Supporting Information for a detailed discussion). The X-ray structure shows the trimer adopting a zigzag conformation in which the *i* and the *i*+2 side chains are oriented on the same side of the backbone, whereas the *i*+1 benzyl group points in the opposite direction.

On the first view, the *cis* preference of α -aminoxy peptoids is somewhat surprising keeping in mind that α -aminoxy peptides preferentially adopt *trans*-amide bonds.^[26] However, we and others showed that the secondary structure in α -aminoxy peptides is primarily stabilized by eight-membered ring hydrogen bonds between the C=O_{*i*} and the N–H_{*i*+2} moieties, which are not possible in the case of α -aminoxy peptoids.^[19,20,26] Thus, in order to further investigate the *cis*-amide preference in α -aminoxy peptoids, we performed a natural bond orbital (NBO) analysis on all-methyl model α -aminoxy peptoids in *cis*- and *trans*-amide configurations (Figures 4A and B) as well as the *cis*-amide α -aminoxy tripeptoid **9** (Figure 4C).

For the model α -aminoxy peptoid in a *cis*-amide configuration, the NBO analysis revealed $\text{C}\alpha_{i-1}\text{H}\cdots\text{O}=\text{C}_{i+1}$ donor–acceptor interactions, which results in an eight-membered δ turn according to the classification by Toniolo and Benedetti^[27] (Figure 4A); the second-order perturbation theory analysis in the NBO basis revealed a mean donor–acceptor stabilization energy of $1.56 \text{ kcal mol}^{-1}$ (Figures 4A and S9A in the Supporting Information). The $\text{C}\alpha$ hydrogen atom involved in the $\text{C}\alpha$ -

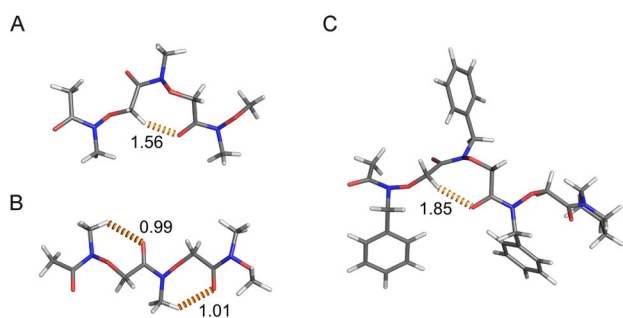


Figure 4. Results from the natural bond orbital analysis. A,B) HF/6-31G*-optimized structures from an all-methyl model compound in a A) *cis* and B) *trans* configuration. C) HF/6-31G*-optimized structure of the α -aminoxy tripeptoid **9** in a *cis* configuration. In A–C) the orange dotted lines depict donor–acceptor interactions. The labels depict the donor–acceptor stabilization energies (in [kcal mol⁻¹]) averaged over the two respective oxygen lone pairs, determined by the second-order perturbation theory analysis.

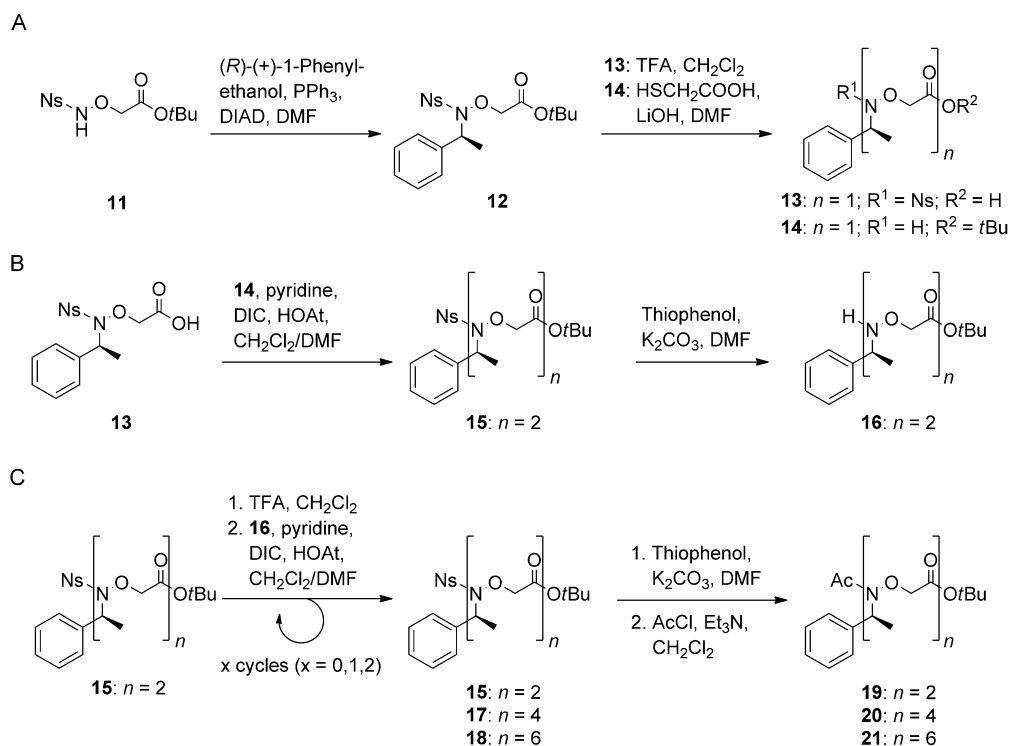
H \cdots O=C interaction is more electron deficient than the geminal, non-involved hydrogen atom (0.2458 au in C α –H \cdots O=C vs. 0.2281 au in C α –H; Figure S9A in the Supporting Information), indicating that electrons are delocalized through the C α –H \cdots O=C interaction. The stabilization energy computed herein is close to the absolute value of the lower limit of the electronic association energy D_e of 2.1 kcal mol⁻¹ computed for *N,N*-dimethylformamide dimers associated through C–H \cdots O=C hydrogen bonds.^[28] The C α \cdots O distance of 3.1 Å coincides with expectations of distances of weak hydrogen bonds.^[29] As to the *trans* configuration, no C α –H \cdots O=C interaction was revealed by

the NBO analysis but rather a C_{*i*}–H \cdots O=C_{*i*} interaction within the same residue (Figure 4B); the latter interaction (stabilization energy: \approx 1.00 kcal mol⁻¹) is weaker than the C α _{*i*}–H \cdots O=C_{*i+1*} one (Figures 4A and B as well as S9A and B in the Supporting Information).

In agreement with results from the all-methyl model peptoid in the *cis* configuration, the NBO analysis also revealed the eight-membered δ turn in the *cis*-amide α -aminoxy tripeptoid **9** (Figure 4C). Herein, the donor–acceptor stabilization energy is stronger than in the model peptoid (1.85 kcal mol⁻¹ in compound **9** vs. 1.56 kcal mol⁻¹ in the model peptoid; Figures 4A and C as well as S9A and C in the Supporting Information). This might be explained by the electron-pushing effect of the benzyl side chains, leading to the amide oxygen atom being more negatively charged (-0.7269 au for compound **9** vs. -0.6980 au for the model peptoid; Figures S9A and C in the Supporting Information).

Taken together, by means of NBO calculations, we found stabilizing donor–acceptor interactions for both the *cis* and *trans* configurations. The formation of an eight-membered δ turn between the residues *i* \rightarrow *i+1* in the *cis* configuration is accompanied by a favorable stabilization energy for C α _{*i*}–H \cdots O=C_{*i+1*} interactions, which could explain the *cis*-amide bond preference for α -aminoxy peptoids. Note that, to the best of our knowledge, no unambiguous report has become available so far for the occurrence of a δ turn in a linear peptide.^[30]

To gain further insight into the potential folding propensities of oligomers we decided to synthesize oligomers featuring α -chiral side chains (Scheme 1). Circular dichroism (CD) spec-



Scheme 1. Synthesis of the α -aminoxy peptoids **19–21** containing α -chiral aromatic side chains (Ns = 2-nitrobenzenesulfonyl, *t*Bu = *tert*-butyl, DIAD = diisopropyl azodicarboxylate, TFA = trifluoroacetic acid, DIC = diisopropylcarbodiimide, Ac = acetyl).

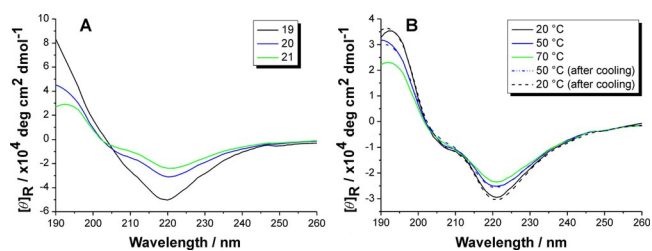


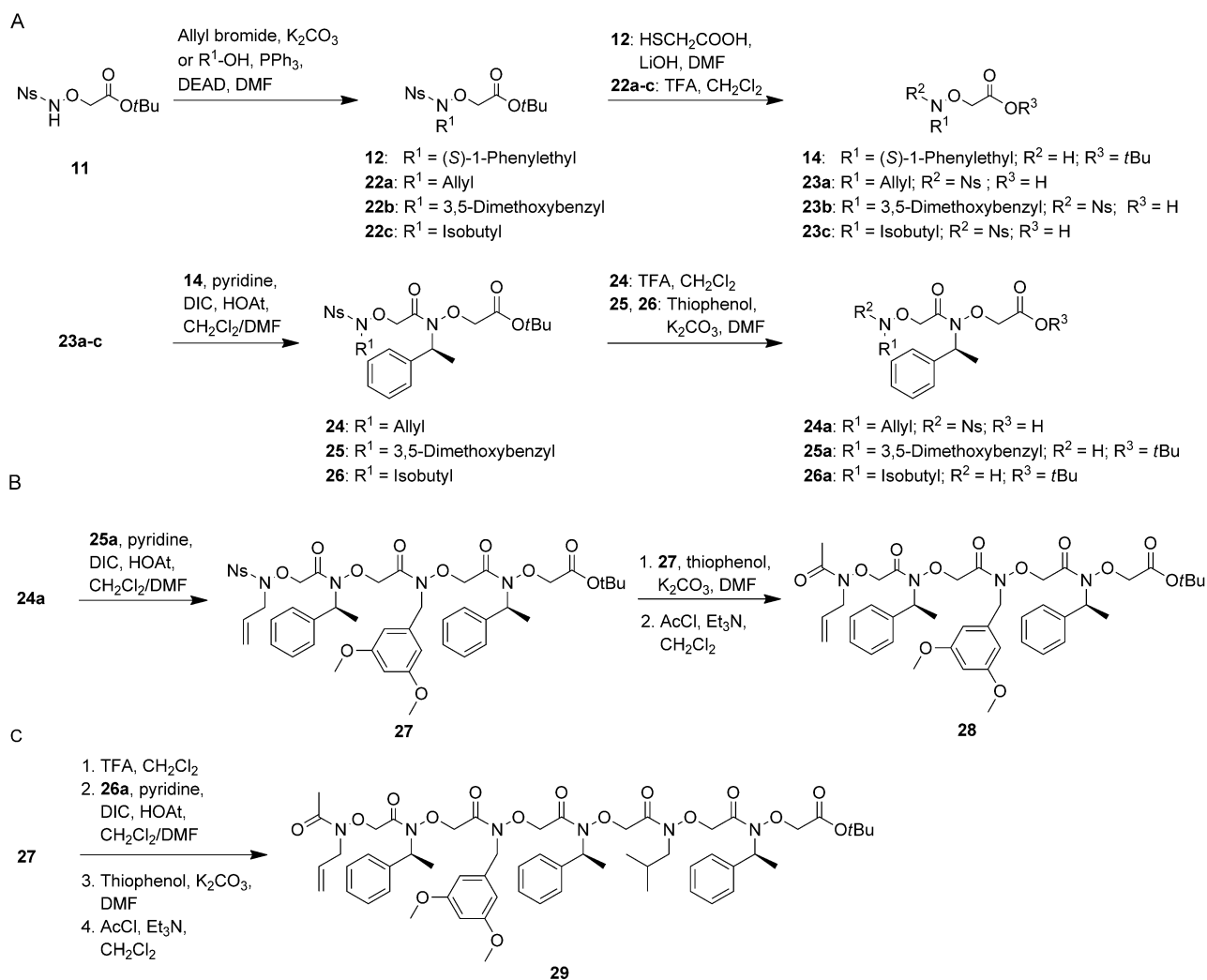
Figure 5. A) CD spectra of compounds **19–21** in acetonitrile (50 μM) at 25 $^{\circ}\text{C}$. B) CD spectra of compound **21** at varying temperatures in acetonitrile (50 μM) (data are expressed in terms of per-residue molar ellipticity (in $[\text{deg cm}^2 \text{dmol}^{-1}]$)).

trospectroscopy has been extensively used to study the secondary structure of α -peptoids. Figure 5 shows the CD spectra of the α -aminoxy peptoids **19–21** in acetonitrile. The CD spectra of compounds **19–21** reveal a characteristic minimum around $\lambda = 220$ nm. Somewhat surprisingly, the intensity of the minimum near $\lambda = 220$ nm decreased with an increasing chain length of the α -aminoxy peptoids. This phenomenon might indicate that this signal is not caused by secondary structure formation but is related to the *N*-(*S*)-1-phenylethyl-containing amide motif itself.^[11,15] To verify this hypothesis we synthesized an acetylated monomer containing the *N*-(*S*)-1-phenylethyl group (see the Supporting Information). The CD spectrum of this α -chiral monomer disclosed a strong minimum at around $\lambda = 220$ nm (Figure S10 in the Supporting Information). Based on this result it appears unlikely that the minimum at $\lambda = 220$ nm is related to secondary structure formation as simple monomers would not be expected to adopt an ordered conformation. On the other hand, starting at the length of a tetramer a shoulder appeared at $\lambda = 209$ nm. It could be speculated that this minimum at $\lambda = 209$ nm might be indicative of a length-dependent secondary structure formation. Because characteristic CD signals do not necessarily need to be indicative of a folding event,^[31] further studies on longer oligomers will be required to investigate the nature of the minimum near $\lambda = 209$ nm in more detail. However, to study the thermostability of the observed CD spectral bands, we collected CD spectra of the hexamer **21** at temperatures in the temperature range 20–70 $^{\circ}\text{C}$. As can be seen in Figure 5B, the hexamer **21** shows only a small reduction in the ellipticity and no change in the shape until 70 $^{\circ}\text{C}$, denoting the thermal stability of the CD spectral bands.

It is not possible to identify the secondary structure of novel peptidomimetics in solution by solely analyzing CD spectra. We therefore designed and synthesized the tetramer **28** and the hexamer **29** in order to perform additional conformational studies. Based on the X-ray analysis of the tripeptoid **9**, we speculated that α -aminoxy peptoids can adopt a conformation in which the *i*, *i*+2, and *i*+4 side chains are located on one side of the peptoid face, whereas the *i*+1, *i*+3, and *i*+5 side chains are located on the opposite side. Thus, we designed the hexamer **29** containing α -chiral, aromatic side chains at the *i*+1, *i*+3, and *i*+5 positions to create an “aromatic face”, which is known to stabilize peptoid helices.^[32] Three structurally diverse side chains were chosen for the *i*, *i*+2, and *i*+4 in order to minimize overlapping NMR signals. The tetramer **28** repre-

sents a simplified and truncated analogue of compound **29**. The synthesis of the oligomers **28** and **29** is outlined in Scheme 2 (see the Supporting Information for synthetic details). Briefly, we prepared a set of dimeric building blocks (Scheme 2A), which were subsequently assembled to the desired oligomers by amide coupling reactions followed by deprotection and acetylation of the *N*-terminal aminoxy moiety (Schemes 2B and C). We conducted 2D NOESY experiments on compounds **28** and **29** to gain further insights into the amide bond geometry and the secondary structure of oligomeric α -aminoxy peptoids. When analyzing the tetramer **28** we observed a strong cross peak between the *N*-terminal acetyl group and the backbone methylene group of the *N*-terminal monomer (*i*) as well as a strong cross peak between the backbone protons of the monomers *i*+2 and *i*+3 indicating a *cis*-amide geometry for the C- and *N*-terminal amide bonds (Figure S11 in the Supporting Information). However, no cross peaks could be observed for the internal amides. Moreover, no further distinct inter-residue NOEs could be detected. In the case of the hexamer **29**, a clear NOE was found for the C-terminal amide suggesting a *cis*-amide geometry (Figure S12 in the Supporting Information). Unfortunately, no inter-residual NOESY cross peaks could be detected. This issue was further investigated by a proton inversion-recovery experiment (Table S2 in the Supporting Information), revealing significant differences in the longitudinal relaxation times of backbone and side-chain protons, which can affect cross relaxation. Notably, a VT NMR experiment on compound **28** revealed no indications for the presence of *cis/trans*-amide bond rotamers (Figure S13 in the Supporting Information). The CD spectra of compounds **28** and **29** in acetonitrile (Figure S14 in the Supporting Information) look very similar when compared to the spectra of compounds **19–21** (Figure 5).

Because our CD and NMR data are insufficient to verify the presence of distinct secondary structures, we performed comprehensive computational studies to investigate the conformational preferences of α -aminoxy peptoids and their potential as helix mimetics. The backbone torsion angles φ , θ , ω , and ψ (Figure 2) are critical for an accurate description of the conformational preferences. We parameterized φ and θ for molecular dynamics (MD) simulations at the molecular mechanics level based on ab-initio calculations (Figures 2 and S15 in the Supporting Information). Fitting of the molecular mechanics energy against the ab-initio energy for the angles φ and θ provided very good correlations [$R^2 \geq 0.95$ (Figure S15 in the Supporting Information)]. For the backbone torsion angles ω and ψ (Figure 2), molecular mechanics energies using the parameters of the GAFF force field (see the Supporting Information) already yielded a very good agreement with the ab-initio energies [$R^2 = 0.99$ (Figure S16 in the Supporting Information)]. The energy minima identified for the torsion potentials of the angles φ , θ , ω , and ψ showed good agreement with the torsion angles found in the crystal structure of the α -aminoxy peptoids **1** and **9** (Figures S15 and S16 as well as Table S3 in the Supporting Information). Hence, the torsion angle parameters accurately reproduce the relative energies of the backbone dihedral angles of α -aminoxy peptoids.



Scheme 2. Synthesis of the tetramer **28** and the hexamer **29** (DEAD = diethyl azodicarboxylate, HOAt = 1-hydroxy-7-azabenzotriazole).

Subsequently, we performed MD simulations of the α -aminoxy peptoids **1** (3.5 μs length), **2** and **3** (3 μs length each), and **9** (3.5 μs length) in explicit chloroform. Choosing this solvent allows for a direct comparison of the simulation results with the NMR data (see above). The MD simulations reached equilibrium with respect to conformational preferences of the angles φ , θ , and ψ , as indicated by highly symmetric torsion angle distributions (Figures S17, S18, and S19 in the Supporting Information) and frequent transitions between energetically preferred states (Figures S20, S21, and S22 in the Supporting Information). In contrast, for the α -aminoxy peptoids **1**, **2**, or **3** started either with a *cis*- or *trans*-amide conformation, a transition in the ω torsion angle between the two conformers was not observed, which is in line with an energetic barrier separating the two conformers (Figure S16 in the Supporting Information for the *N*-ethoxyformamide model compound; Figure S23 in the Supporting Information for the α -aminoxy peptoid **30** (*N,N*-dimethyl-2-((*N*-methylacetamido)-oxy)acetamide) for probing the effect of an acetyl cap group and an *N*-methyl side chain) and previous work.^[33] In addition, our calculations show that the *cis* conformer is preferred over the *trans* conformer by

approximately 2.8 kcal mol⁻¹ for peptoid **30**, whereas the *cis* and *trans* conformers are virtually isoenergetic for the *N*-ethoxyformamide model compound (Figures S23 and S16 in the Supporting Information, respectively), which is consistent with *cis/trans* energy differences of up to 1.4 kcal mol⁻¹ in regular (not α -aminoxy) peptoids, as reported by Yoo and Kirshenbaum.^[9] These findings also agree with the above-described NMR experiments and the crystal structure analyses. Finally, the distributions of the backbone torsion angles of the monomeric α -aminoxy peptoids **1**, **2**, and **3** observed in the MD simulations showed a very good to good agreement with the torsion angle values found in the crystal structures of the α -aminoxy peptoids **1** and **9** (Figures S17, S18, and S19 as well as Table S3 in the Supporting Information). The relative free energies of the α -aminoxy peptoid **1** as a function of the backbone dihedral angles φ , θ , and ψ computed from the frequency of occurrence of the conformations during the MD simulations allowed us to identify the preferred backbone conformations of the α -aminoxy peptoid **1** (Figure S24 in the Supporting Information); given the almost identical torsion angle distributions (Figures S17, S18, and S19 in the Supporting Information), simi-

lar conformations are expected to be favorable also for the other α -aminoxy peptoids. The lack of mirror symmetry in the θ/φ and θ/ψ projections of the relative free energy is compatible with the observation that the amide nitrogen atom shows a certain degree of pyramidalization, which is in agreement with findings of Jordan and co-workers, leading to a transient chirality.^[33] Superimposing the low-energy conformations of the α -aminoxy peptoids **1**, **2**, and **3** extracted from the respective MD simulations onto the crystal structure of the α -aminoxy peptoid **1** results in backbone-atom root mean square deviations (RMSD) ≤ 0.6 Å (Figure 6A–C). Similarly, overlaying a low-energy conformation of the α -aminoxy peptoid **9** onto the crystal structure of the same compound results in a backbone-atom RMSD value of 1.2 Å (Figure 6D). These results show that the MD simulations yield low-energy conformations of α -aminoxy peptoids that are in very good agreement with the experimentally determined structures.

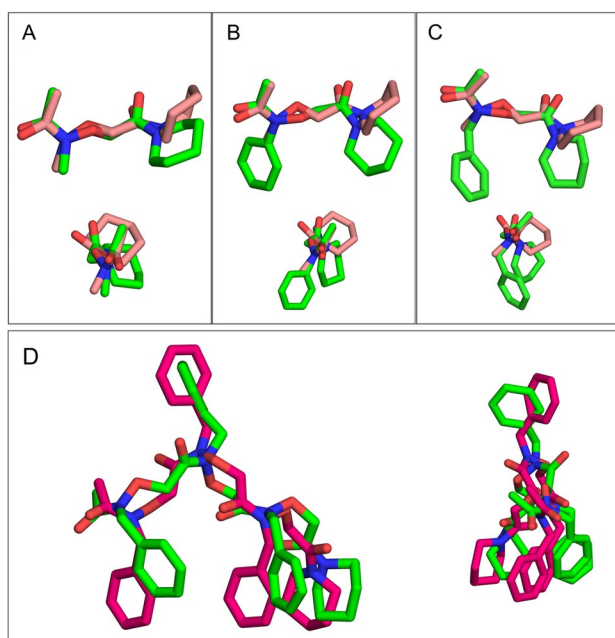


Figure 6. A–C) Overlay of the low-energy conformations of the α -aminoxy peptoids **1**, **2**, and **3** obtained from MD simulations (green) onto the crystal structure of the α -aminoxy peptoid **1** (pink), resulting in RMSD values of the backbone atoms of 0.57, 0.60, and 0.59 Å for compounds **1**, **2**, and **3**, respectively. In the lower panel, the overlays are rotated by 90°. D) Overlay of a low-energy conformation of the α -aminoxy peptoid **9** obtained from MD simulations (green) onto the crystal structure of the α -aminoxy peptoid **9** (magenta), resulting in an RMSD value of the backbone atoms of 1.2 Å. In the right panel, the overlay is rotated by 90°.

We used the thus validated setup of MD simulations to investigate the conformational properties of the more complex tetrameric (compound **28**) and hexameric (compound **29**) α -aminoxy peptoids. MD simulations of compounds **28** (3.5 μ s length) and **29** (2 μ s length) in explicit chloroform again yielded distributions of backbone torsion angles that are in very good agreement with the values of the crystal structures of the α -aminoxy peptoids **1** and **9**, and are similar to those obtained with the α -aminoxy peptoids **1**, **2**, and **3** (data not

shown). The conformational ensembles obtained by the MD simulations of the α -aminoxy peptoids **28** and **29** were clustered according to the RMSD values. The four most populated clusters that account for 71% (for the α -aminoxy peptoid **28**) and 64% (for the α -aminoxy peptoid **29**) of the MD ensembles were further analyzed. Overlaying the C β atoms of the α -aminoxy peptoid **28** onto the C β atoms of a canonical α -helix shows that the α -aminoxy peptoid scaffold can closely mimic the spatial arrangement of the peptide side chains at the positions i , $i+1$, $i+3$, and $i+5$. When the N terminus of the peptoid is oriented toward the C terminus of the helix, the RMSD value of the coordinates of the respective atom pairs is 0.5 Å (Figure 7A). When the peptoid is oriented in the opposite direction, the RMSD value is 0.7 Å (Figure 7B). Overlaying the C β atoms of the peptoid **29** with the C β atoms of a canonical α -helix shows that the α -aminoxy peptoid scaffold can also address an i , $i+2$, $i+3$, $i+5$, $i+7$, $i+11$ amino acid pattern when the N terminus of the peptoid is oriented toward the C terminus of the helix (Figure 7C), and alternatively an i , $i+4$, $i+6$, $i+8$, $i+9$, $i+11$ pattern when the peptoid is oriented in the opposite direction (Figure 7D). The RMSD value of the coordinates of the respective atom pairs is 1.1 Å in both cases. In summary, the conformational analysis based on the MD simulations reveals that α -aminoxy peptoids adopt conformations that can mimic i , $i+1$, $i+3$, $i+5$; i , $i+2$, $i+3$, $i+5$, $i+7$, $i+11$; and i , $i+4$, $i+6$, $i+8$, $i+9$, $i+11$ patterns of substituent orientations with respect to an α -helix.

Conclusion

We have performed the first thorough analysis of the folding propensities of α -aminoxy peptoids. To this end, we designed and synthesized a series of model α -aminoxy peptoids utilizing well-established cap groups to investigate the influence of several side chains on the amide conformation and secondary structure. Interestingly, for α -aminoxy peptoids we observed a unique preference for *cis*-amide bonds in comparison to other peptoid backbones. The formation of an eight-membered δ turn that is stabilized by C α_i -H...O=C $_{i+1}$ interactions between the residues $i \rightarrow i+1$ in the *cis* configuration might explain the *cis*-amide preference of α -aminoxy peptoids. MD simulations suggest that α -aminoxy oligopeptoids can fold into a distinct secondary structure closely mimicking the spatial arrangement of peptide side chains in a canonical α -helix. It is worth noting that α -aminoxy peptoid monomers can be easily prepared from the readily available starting material **11** either by classical alkylation with alkyl halides or by a Mitsunobu reaction. This efficient monomer synthesis may therefore allow for the preparation of α -aminoxy peptoid libraries with a large chemical diversity in the future. Given their ease of synthesis, their structural diversity, and their conformational properties, α -aminoxy peptoids represent a promising new class of peptidomimetic foldamers that may be highly useful in a variety of novel applications such as material sciences and medicinal chemistry. In conclusion, α -aminoxy peptoids were introduced as a new peptoid backbone capable of controlling the amide

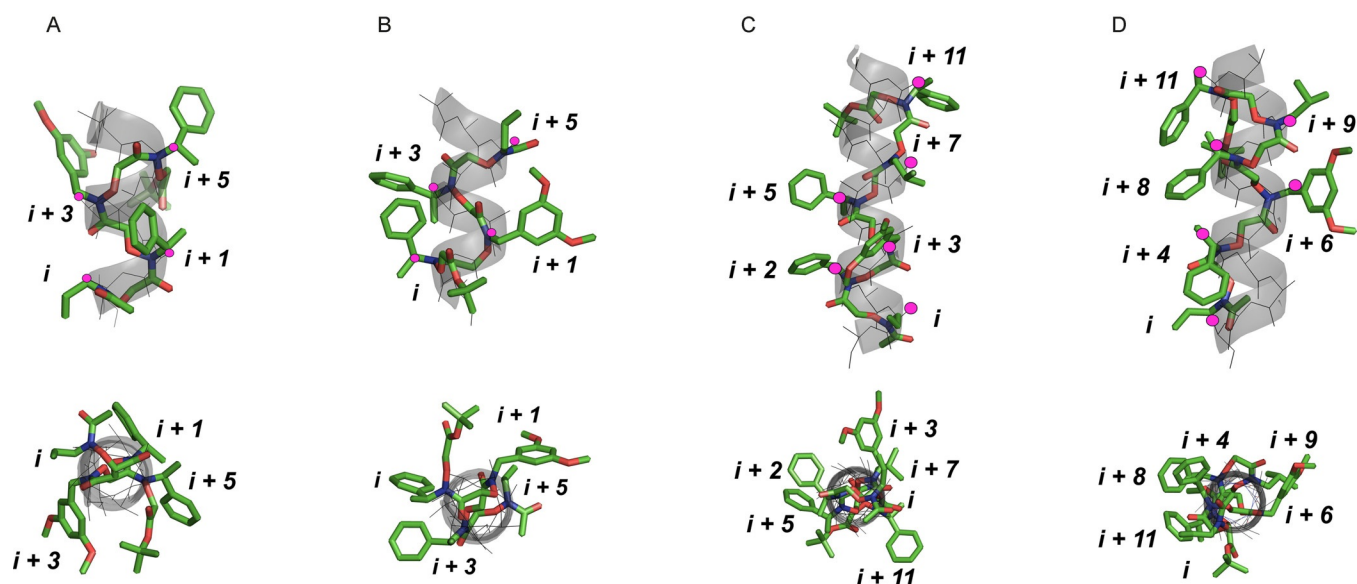


Figure 7. Overlay of the C β atoms of low-energy conformations of the α -aminoxy peptoids **28** (A and B) and **29** (C and D) onto the C β atoms of a canonical α -helix (indicated by the pink spheres). In the case of the α -aminoxy peptoid **28**, the scaffold can closely mimic the spatial arrangement of the peptide side chains at the positions i , $i+1$, $i+3$, $i+5$, with an RMSD value of the coordinates of the respective atom pairs of 0.5 Å when the N terminus of the α -aminoxy peptoid is oriented toward the C terminus of the helix, and of 0.7 Å when the α -aminoxy peptoid is oriented in the opposite direction (A and B, respectively). In the case of the α -aminoxy peptoid **29**, the scaffold can closely mimic the spatial arrangement of peptide side chains at the positions i , $i+2$, $i+3$, $i+5$, $i+7$, $i+11$ when the N terminus of the α -aminoxy peptoid is oriented toward the C terminus of the helix (C), and the positions i , $i+4$, $i+6$, $i+8$, $i+9$, $i+11$ when the α -aminoxy peptoid is oriented in the opposite direction (D), with an RMSD value of 1.1 Å in both cases.

isomerism while maintaining the potential for side-chain diversity.

Experimental Section

See the Supporting Information for experimental details. CCDC 1508156 (**1**) and 1508157 (**9**) contain the supplementary crystallographic data for this paper. These data can be obtained free of charge from The Cambridge Crystallographic Data Centre via www.ccdc.cam.ac.uk/data_request/cif.

Acknowledgements

This work was supported by funds from the Fonds der Chemischen Industrie (to F.K.H.). The Deutsche Forschungsgemeinschaft (DFG) is acknowledged for funds used to purchase the UHR-TOF maXis 4G, Bruker Daltonics, Bremen HRMS instrument used in this research. Financial support by the Deutsche Forschungsgemeinschaft (DFG) for funds (INST 208/704-1 FUGG to H.G.) to purchase the hybrid computer cluster used in this study is gratefully acknowledged. Computational support and infrastructure was provided by the "Center for Information and Media Technology" (ZIM) at the Heinrich Heine University Düsseldorf (HHU). We thank the Institute of Physical Biology at the HHU for providing us access to the CD spectrometer.

Keywords: aminoxy peptoids • conformational analysis • foldamers • peptidomimetics • peptoids

[1] S. M. Miller, R. J. Simon, S. Ng, R. N. Zuckermann, J. M. Kerr, W. H. Moos, *Bioorg. Med. Chem. Lett.* **1994**, *4*, 2657–2662.

- [2] Y.-U. Kwon, T. Kodadek, *J. Am. Chem. Soc.* **2007**, *129*, 1508–1509.
 [3] M. M. Reddy, K. Bachhawat-Sikder, T. Kodadek, *Chem. Biol.* **2004**, *11*, 1127–1137.
 [4] P. G. Alluri, M. M. Reddy, K. Bachhawat-Sikder, H. J. Olivos, T. Kodadek, *J. Am. Chem. Soc.* **2003**, *125*, 13995–14004.
 [5] T. Hara, S. R. Durell, M. C. Myers, D. H. Appella, *J. Am. Chem. Soc.* **2006**, *128*, 1995–2004.
 [6] I. M. Mándity, F. Fülöp, *Expert Opin. Drug Discovery* **2015**, *10*, 1163–1177.
 [7] S. Suwal, T. Kodadek, *Org. Biomol. Chem.* **2013**, *11*, 2088–2092.
 [8] J. A. Hodges, R. T. Raines, *Org. Lett.* **2006**, *8*, 4695–4697.
 [9] B. Yoo, K. Kirshenbaum, *Curr. Opin. Chem. Biol.* **2008**, *12*, 714–721.
 [10] C. Baldauf, R. Günther, H.-J. Hofmann, *Phys. Biol.* **2006**, *3*, S1–S9.
 [11] A. S. Norgren, S. Zhang, P. I. Arvidsson, *Org. Lett.* **2006**, *8*, 4533–4536.
 [12] C. A. Olsen, M. Lambert, M. Witt, H. Franzyk, J. W. Jaroszewski, *Amino Acids* **2008**, *34*, 465–471.
 [13] C. A. Olsen, H. L. Ziegler, H. M. Nielsen, N. Frimodt-Møller, J. W. Jaroszewski, H. Franzyk, *ChemBioChem* **2010**, *11*, 1356–1360.
 [14] O. Roy, S. Faure, V. Thery, C. Tallefumier, *Org. Lett.* **2008**, *10*, 921–924.
 [15] J. S. Laursen, P. Harris, P. Fristrup, C. A. Olsen, *Nat. Commun.* **2015**, *6*, 7013.
 [16] J. S. Laursen, J. Engel-Andreasen, P. Fristrup, P. Harris, C. A. Olsen, *J. Am. Chem. Soc.* **2013**, *135*, 2835–2844.
 [17] C. Caumes, O. Roy, S. Faure, C. Tallefumier, *J. Am. Chem. Soc.* **2012**, *134*, 9553–9556.
 [18] I. Shin, K. Park, *Org. Lett.* **2002**, *4*, 869–872.
 [19] X. Li, Y.-D. Wu, D. Yang, *Acc. Chem. Res.* **2008**, *41*, 1428–1438.
 [20] X. Li, D. Yang, *Chem. Commun.* **2006**, *32*, 3367–3379.
 [21] N. H. Shah, G. L. Butterfoss, K. Nguyen, B. Yoo, R. Bonneau, D. L. Rabenstein, K. Kirshenbaum, *J. Am. Chem. Soc.* **2008**, *130*, 16622–16632.
 [22] a) B. H. Meier, R. R. Ernst, *J. Am. Chem. Soc.* **1979**, *101*, 6441–6442; b) C. L. Perrin, T. J. Dwyer, *Chem. Rev.* **1990**, *90*, 935–967.
 [23] D. X. Hu, P. Grice, S. V. Ley, *J. Org. Chem.* **2012**, *77*, 5198–5202.
 [24] All ratios were calculated by integrating and averaging at least three ^1H NMR signals at 15 mM concentration.
 [25] P. Le Grel, A. Salaün, C. Mocquet, B. L. Grel, T. Roisnel, M. Potel, *J. Org. Chem.* **2011**, *76*, 8756–8767.

- [26] a) D. Diedrich, A. J. Rodrigues Moita, A. R  ther, B. Frieg, G. J. Reiss, A. Hoepfner, T. Kurz, H. Gohlke, S. L  deke, M. U. Kassack, F. K. Hansen, *Chem. Eur. J.* **2016**, *22*, 17600–17611; b) B. Draghici, F. K. Hansen, A.-M. Buciumas, B. E.-D. M. El-Gendy, E. Todadze, A. R. Katritzky, *RSC Adv.* **2011**, *1*, 602–606; c) D. Yang, G. J. Liu, Y. Hao, W. Li, Z. M. Dong, D. W. Zhang, N. Y. Zhu, *Chem. Asian J.* **2010**, *5*, 1356–1363.
- [27] C. Toniolo, E. Benedetti, *Crit. Rev. Biochem.* **1980**, *9*, 1–44.
- [28] R. Vargas, J. Garza, D. A. Dixon, B. P. Hay, *J. Am. Chem. Soc.* **2000**, *122*, 4750–4755.
- [29] C. Bissantz, B. Kuhn, M. Stahl, *J. Med. Chem.* **2010**, *53*, 5061–5084.
- [30] C. Toniolo, M. Crisma, A. Moretto, C. Peggion, F. Formaggio, C. Alem  n, C. Catiuela, C. Ramakrishnan, P. Balaram, *Chem. Eur. J.* **2015**, *21*, 13866–13877.
- [31] A. Gl  ttli, X. Daura, D. Seebach, W. F. van Gunsteren, *J. Am. Chem. Soc.* **2002**, *124*, 12972–12978.
- [32] C. W. Wu, T. J. Sanborn, K. Huang, R. N. Zuckermann, A. E. Barron, *J. Am. Chem. Soc.* **2001**, *123*, 6778–6784.
- [33] P. A. Jordan, B. Paul, G. L. Butterfoss, P. D. Renfrew, R. Bonneau, K. Kirshenbaum, *Biopolymers* **2011**, *96*, 617–626.

Manuscript received: November 1, 2016

Accepted Article published: January 16, 2017

Final Article published: February 13, 2017
